Supplement of Atmos. Chem. Phys., 25, 5175–5197, 2025
https://doi.org/10.5194/acp-25-5175-2025-supplement

Atmospheric Chemistry and Physics
Open Access

Supplement of

Trends and drivers of soluble iron deposition from East Asian dust to the Northwest Pacific: a springtime analysis (2001–2017)

Hanzheng Zhu et al.

Correspondence to: Xinyi Dong (dongxy@nju.edu.cn)

Table S1. List of irreversible heterogeneous reactions about Ca. (Zaveri et al., 2008)

	Irreversible heterogeneous reactions
R1	$CaCO_3(s) + H_2SO_4(g) \rightarrow CaSO_4(s) + H_2O(g) + CO_2(g)$
R2	$CaCl2(s,l) + H_2SO_4\ (g) \rightarrow CaSO_4(s) + 2HNO_3(g)$
R3	$Ca(NO_3)_2(s,l) + + H_2SO_4(g) \rightarrow CaSO_4(s) + 2HCl(g)$
R4	$CaCO_3(s) + 2HNO_3(g) \rightarrow Ca(NO_3)_2(s) + H_2O(g) + CO_2(g)$
R5	$CaCl2(s,l) + 2HNO_3(g) \rightarrow Ca(NO_3)_2(g) + 2HCl(g)$
R6	$CaCO_3(s) + 2HCl(g) \rightarrow CaCl_2(s) + H_2O(g) + CO_2(g)$

Table S2. Iron content and initial iron solubility for each of the five minerals

	Fe_rs	**Fe_ms**	**Fe_ss**	**Fe content**	**Fe solubility**
Hematite	0%	0%	57.5%	57.5%	0%
Smectite	0.55%	10.45%	0%	11.0%	5%
Illite	0.11%	3.89%	0%	4.0%	2.8%
Kaolinite	0.01%	0%	0.23%	0.24%	4.2%
Feldspar	0.01%	0%	0.33%	0.34%	2.9%

Table S3. Global emissions of dust, dust total/soluble iron in 2017.

	Dust	**Total iron**	**Soluble iron**	**Iron content**	**Iron solubility**
Emissions (Tg/yr)	2707	109	0.98	4.0%	0.91%
coarse mode	2677	107	0.93	3.9%	0.88%
fine mode	30	2	0.05	5.3%	3.4%

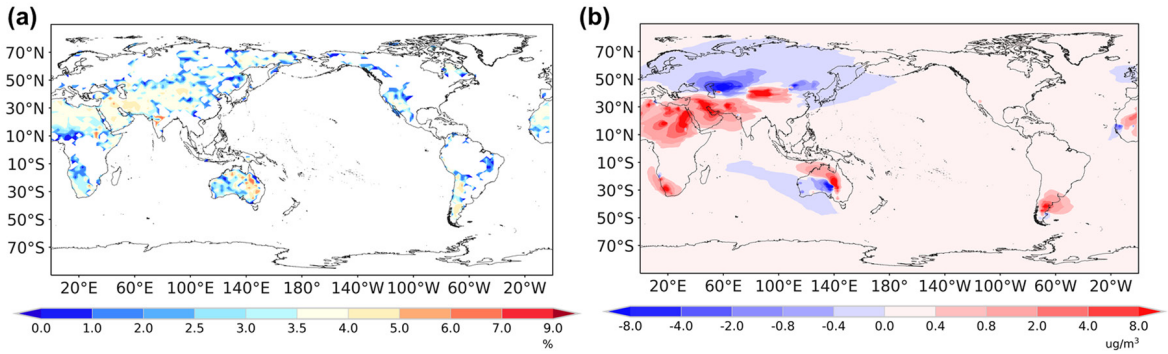

Figure S1. (a) Spatial distribution of iron content in coarse mode dust aerosol. (b) Changes in dust total iron surface concentrations from the developed model compared to the setting of 3.5%, averaged over the 2001-2017 springs.

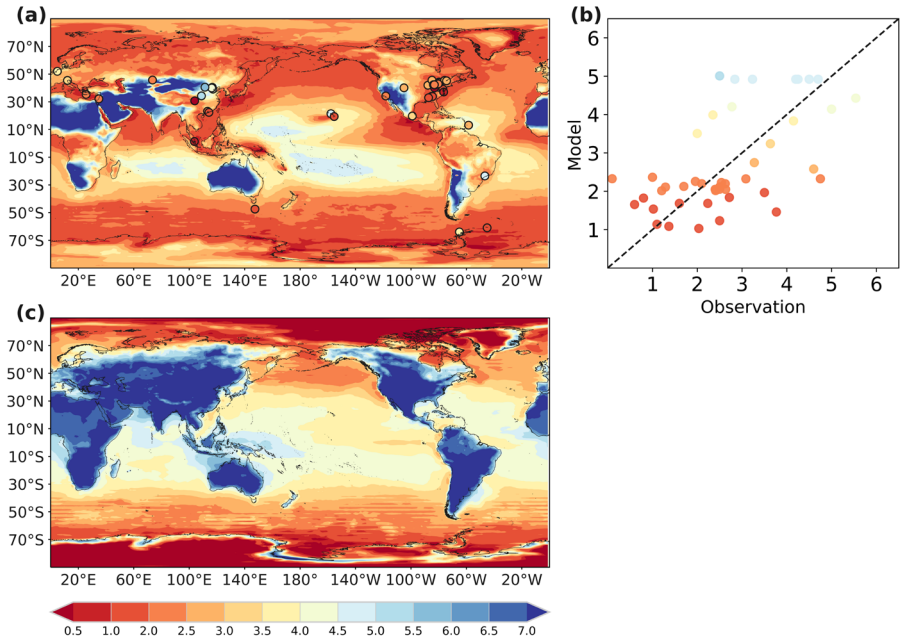

Figure S2. (a) Spatial distribution of surface aerosol pH in accumulation mode in 2013 and observationally estimated ground-level fine-aerosol pH (dots) from Pye et al. (2020). (b) The linear relationship between simulated surface aerosol pH in accumulation mode and observationally estimated ground-level fine-aerosol pH. (c) Spatial distribution of sirface aerosol pH in coarse mode in 2013. The aerosol pH is calculated based on H+ concentrations for each aerosol mode at each time step.

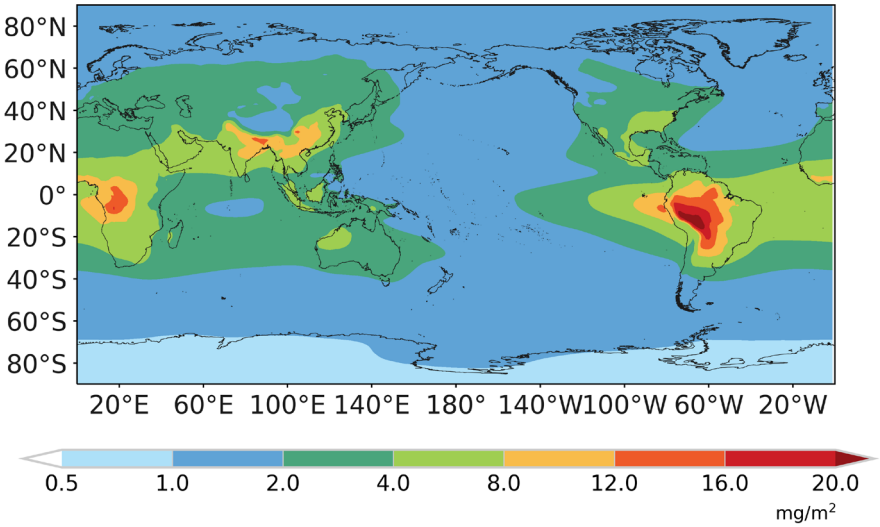

Figure S3. Spatial distribution of Secondary Organic Aerosols (SOA) burden from 2001 to 2017 with simulation data from Liu et al. (2023).

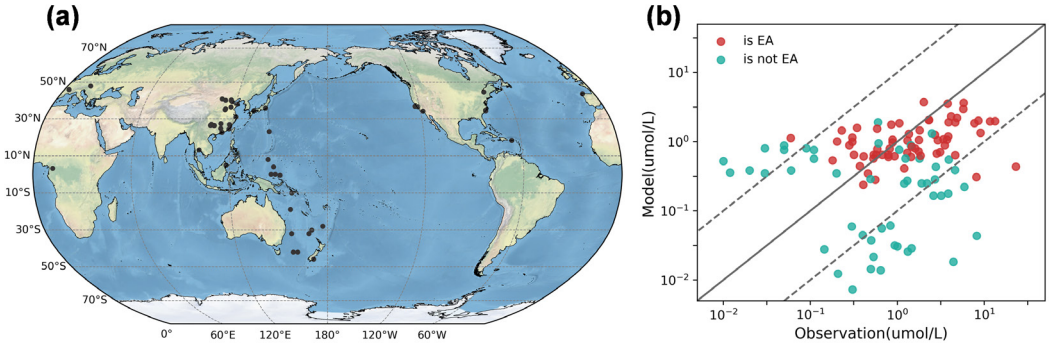

Figure S4. (a) Sample locations of the observed oxalate in rain/cloud water (Sempéré and Kawamura, 1996; Willey et al., 2000; Brooks Avery et al., 2001; Kawamura et al., 2001; Hegg et al., 2002; Kieber et al., 2002; Löflund et al., 2002; Peña et al., 2002; Kim et al., 2003; Sigha-Nkamdjou et al., 2003; Crahan et al., 2004; Hu et al., 2005; Brooks Avery et al., 2006; Xu et al., 2009; Huang et al., 2010; Huo et al., 2010; Sumari et al., 2010; Gioda et al., 2011; Wang et al., 2011; Zhang et al., 2011; Khuntong, 2012; Zhu et al., 2016; Du et al., 2017; Zhao et al., 2019; Zhang et al., 2021; González et al., 2022; Lee et al., 2022; Xie et al., 2022; Sun et al., 2024). (b) The comparison between estimated oxalate concentration in cloud water and observations. Red circles represent locations in East Asia (EA), and green circles represent locations elsewhere.

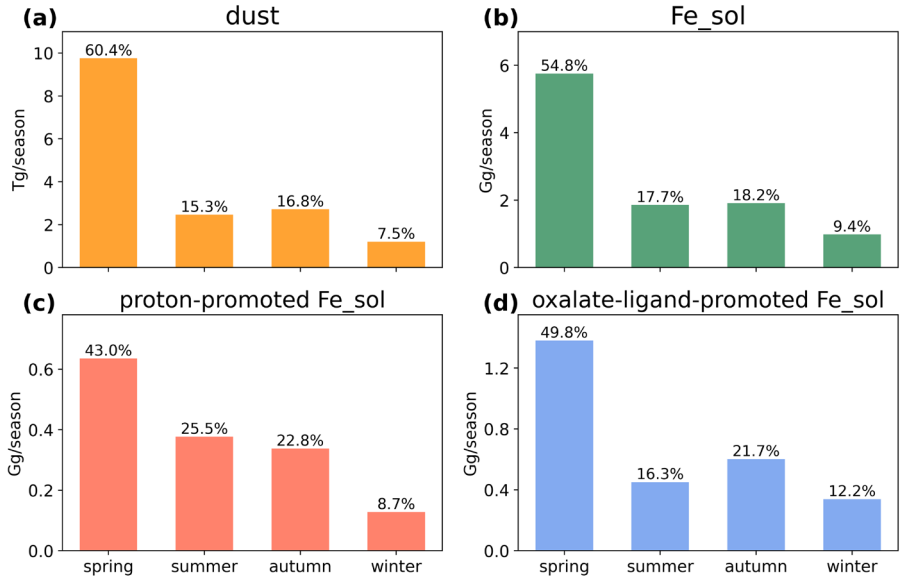

Figure S5. Dust, total soluble iron, proton-promoted soluble iron, and oxalate-promoted soluble iron deposition over Northwest Pacific (30-50N, 140E-160W) in 2001.

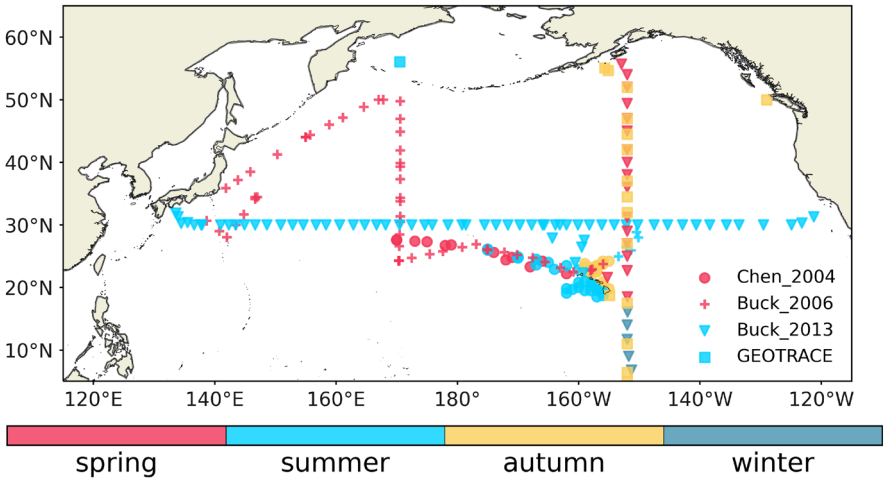

Figure S6. Seasons and locations of total and soluble iron observational samples over the North Pacific. Different colors represent different moths and different shapes represent different data sources (Chen et al., 2004; Buck et al., 2006; Buck et al., 2013; GEOTRACES Intermediate Data Product Group (2021)).

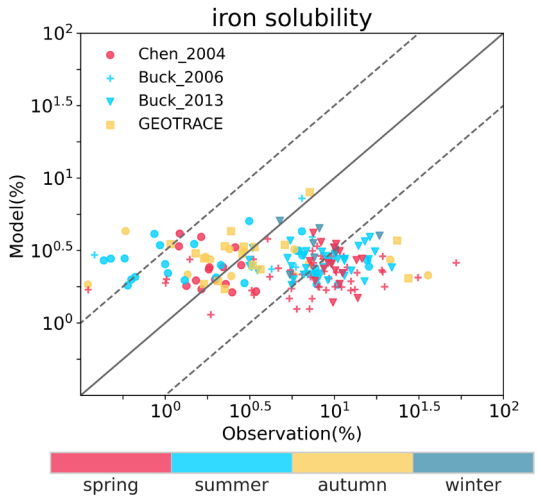

Figure S7. The comparison about iron solubility between simulation and observations.

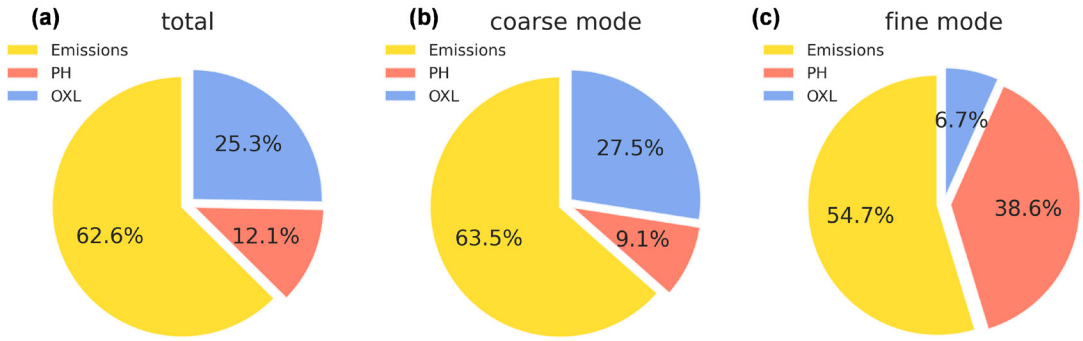

Figure S8. Relative contributions of emissions, oxalate-promoted, and proton-promoted processing to the Northwest Pacific dust soluble iron deposition averaged of 2001-2017 springs in total (a), coarse mode (b), and fine mode (c).

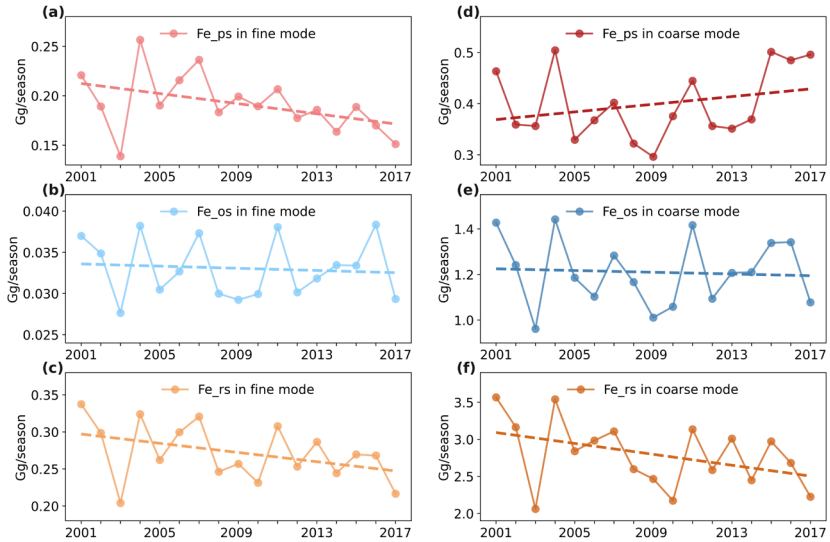

Figure S9. Interannual variations of dust soluble iron deposition from proton-promoted (a, d), oxalate-promoted (b, e) and emissions (c, f) in coarse and fine mode (aitken + accumulation) to the Northwest Pacific averaged of 2001-2017 springs.

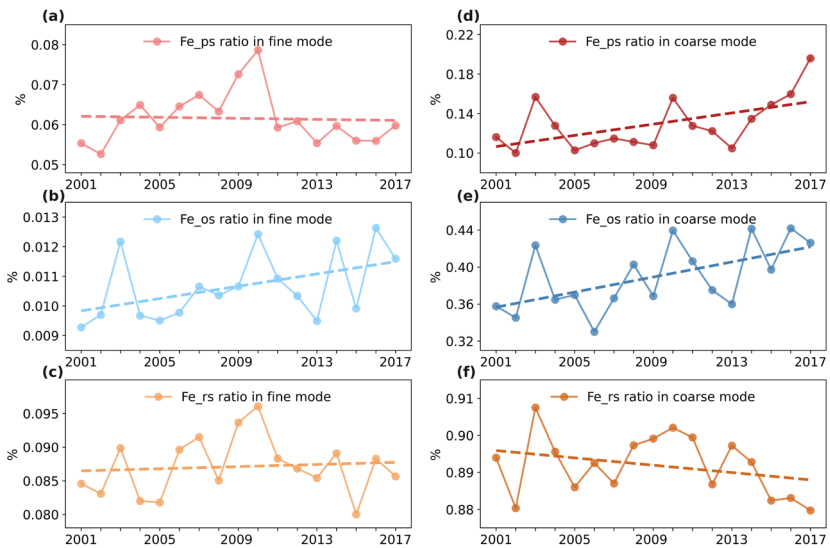

Figure S10. Interannual variations of contribution of each iron solubilization process including proton-promoted (a, d), oxalate-promoted (b, e) and emissions (c, f) in coarse and fine mode (aitken + accumulation) to dust total iron deposition to the Northwest Pacific averaged of 2001-2017 springs.

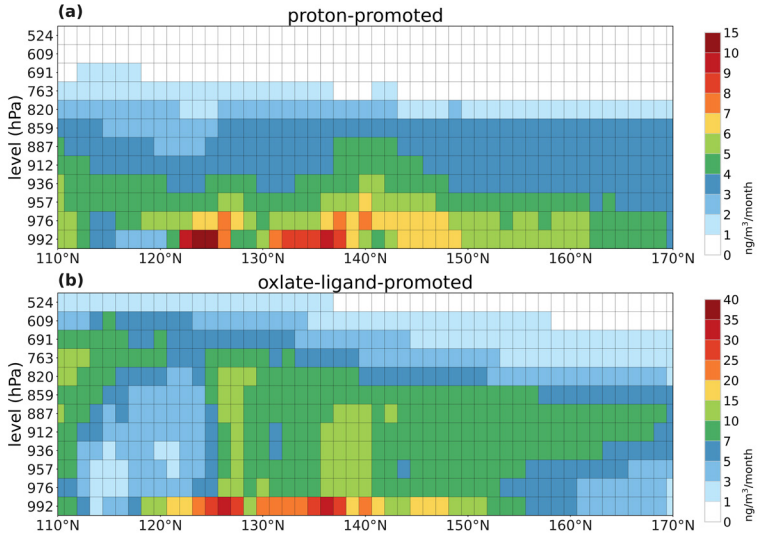

Figure S11. Vertical distributions of proton-promoted (a) and oxalate-promoted (b) soluble iron production rate averaged 30N-50N during the 2001-2017 springs.

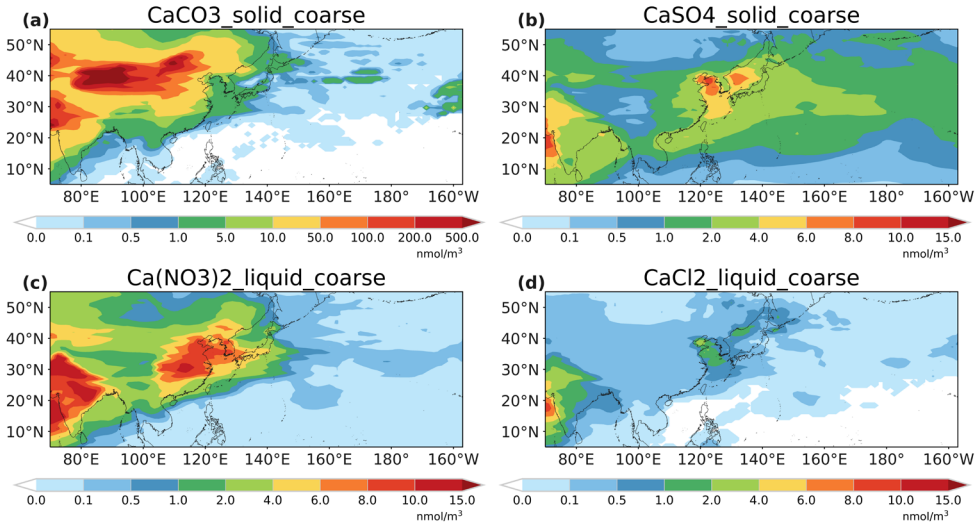

Figure S12. Spatial distributions of coarse mode solid-phase $CaCO_3$(a), solid-phase $CaSO_4$(b), liquid-phase $Ca(NO_3)_2$, and liquid-phase $CaCl_2$ averaged of 2001 spring.

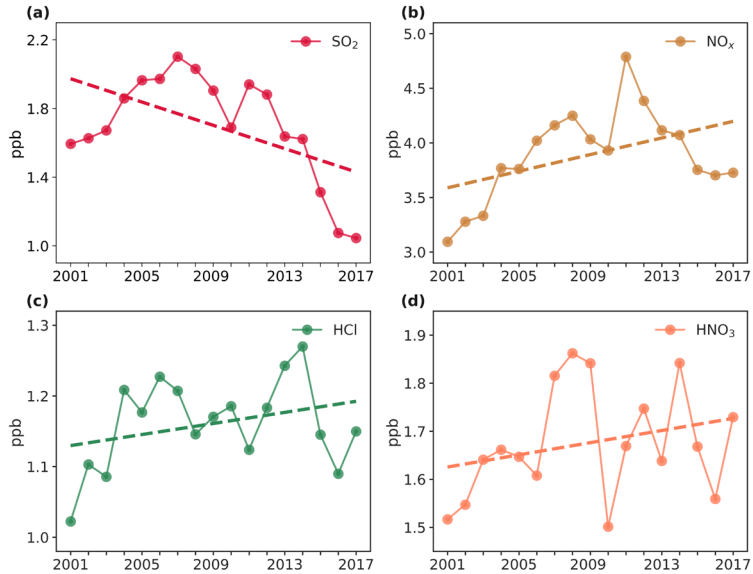

Figure S13. Temporal variations of surface concentrations of SO_2 (a), NO_x (a), HCl (c), and HNO_3(d) over the area of high production rate of proton-promoted soluble iron (30-45N, 120-150E) averaged of 2001-2017 springs.

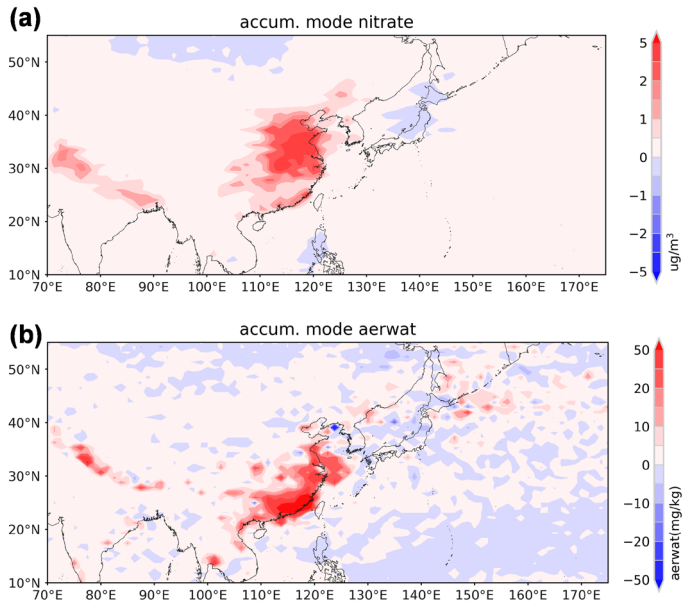

Figure S14. Changes in the spatial distributions of surface accumulation mode nitrate aerosol concentration (a) and aerosol water content (b) induced by NO_x experiment.

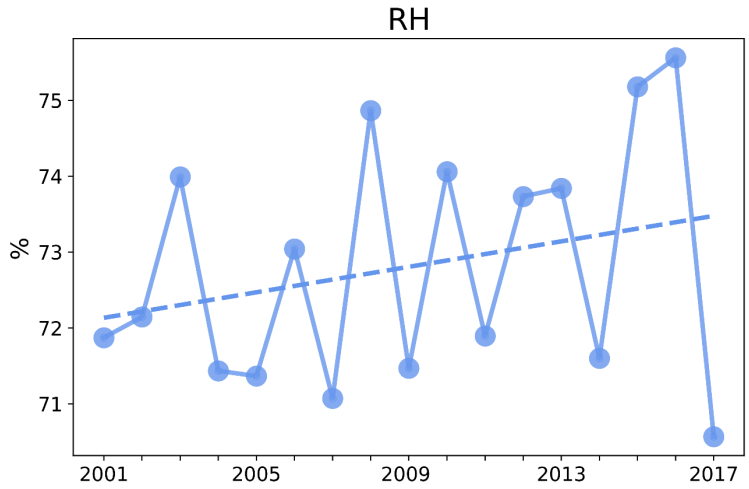

Figure S15. Temporal variations of simulated surface relative humidity over the high production rate of oxalate-promoted soluble iron area (30-45N, 120-150E) averaged of 2001-2017 springs.

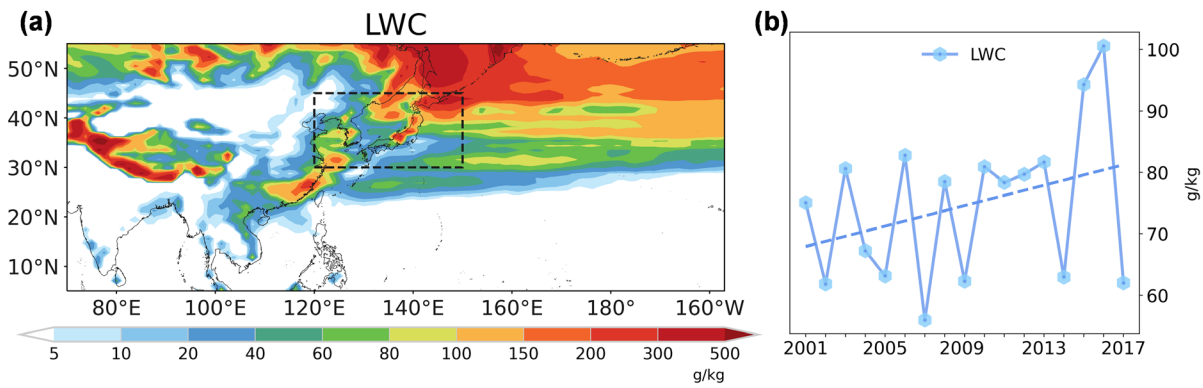

Figure S16. (a) Spatial distributions of surface cloud liquid water content averaged of 2001-2017 springs. (b) Temporal variations of surface cloud liquid water content over high production rate area (30-45N, 120-150E) averaged of 2001-2017 springs.

References

Chen, Y.: Sources and fate of atmospheric nutrients over the remote oceans and their role on controlling marine diazotrophic microorganisms, Doctoral dissertation, available at: https://drum.lib.umd.edu/handle/1903/1967, 2004.

Brooks Avery, G., Willey, J. D., and Kieber, R. J.: Diurnal variations in major rainwater components at a coastal site in North Carolina, Atmospheric Environment, 35, 3927-3933, https://doi.org/10.1016/S1352-2310(01)00202-3, 2001.

Brooks Avery, G., Kieber, R. J., Witt, M., and Willey, J. D.: Rainwater monocarboxylic and dicarboxylic acid concentrations in southeastern North Carolina, USA, as a function of air-mass back-trajectory, Atmospheric Environment, 40, 1683-1693, https://doi.org/10.1016/j.atmosenv.2005.10.058, 2006.

Buck, C. S., Landing, W. M., and Resing, J.: Pacific Ocean aerosols: Deposition and solubility of iron, aluminum, and other trace elements, Marine Chemistry, 157, 117-130, https://doi.org/10.1016/j.marchem.2013.09.005, 2013.

Buck, C. S., Landing, W. M., Resing, J. A., and Lebon, G. T.: Aerosol iron and aluminum solubility in the northwest Pacific Ocean: Results from the 2002 IOC cruise, Geochemistry, Geophysics, Geosystems, 7, https://doi.org/10.1029/2005GC000977, 2006.

Crahan, K. K., Hegg, D., Covert, D. S., and Jonsson, H.: An exploration of aqueous oxalic acid production in the coastal marine atmosphere, Atmospheric Environment, 38, 3757-3764, https://doi.org/10.1016/j.atmosenv.2004.04.009, 2004.

Du, W., Hong, Z., Chen, Y., Deng, J., Chen, J., Xu, L., Hong, Y., and Xiao, H.: Spatiotemporal distribution and source apportionment of low molecular weight organic acids in wet precipitation at a coastal city, China, Environmental Science and Pollution Research, 24, 8399-8410, 10.1007/s11356-017-8498-3, 2017.

GEOTRACES Intermediate Data Product Group (2021). The GEOTRACES Intermediate Data Product 2021 version 2 (IDP2021v2). NERC EDS British Oceanographic Data Centre NOC. doi: 10.5285/ff46f034-f47c-05f9-e053-6c86abc0dc7e.

Gioda, A., Reyes-Rodríguez, G. J., Santos-Figueroa, G., Collett Jr., J. L., Decesari, S., Ramos, M. d. C. K. V., Bezerra Netto, H. J. C., de Aquino Neto, F. R., and Mayol-Bracero, O. L.: Speciation of water-soluble inorganic, organic, and total nitrogen in a background marine environment: Cloud water, rainwater, and aerosol particles, Journal of Geophysical Research: Atmospheres, 116, https://doi.org/10.1029/2010JD015010, 2011.

González, A. G., Bianco, A., Boutorh, J., Cheize, M., Mailhot, G., Delort, A.-M., Planquette, H., Chaumerliac, N., Deguillaume, L., and Sarthou, G.: Influence of strong iron-binding ligands on cloud water oxidant capacity, Science of The Total Environment, 829, 154642, https://doi.org/10.1016/j.scitotenv.2022.154642, 2022.

Hegg, D. A., Gao, S., and Jonsson, H.: Measurements of selected dicarboxylic acids in marine cloud water, Atmospheric Research, 62, 1-10, https://doi.org/10.1016/S0169-8095(02)00023-6, 2002.

Hu, M., Zhang, J., and Wu, Z.: Chemical compositions of precipitation and scavenging of particles in Beijing, Science in China Series B: Chemistry, 48, 265-272, 10.1360/042004-49, 2005.

Huang, X.-F., Li, X., He, L.-Y., Feng, N., Hu, M., Niu, Y.-W., and Zeng, L.-W.: 5-Year study of rainwater chemistry in a coastal mega-city in South China, Atmospheric Research, 97, 185-193, https://doi.org/10.1016/j.atmosres.2010.03.027, 2010.

Huo, M., Sun, Q., Bai, Y., Xie, P., Liu, Z., Li, J., Wang, X., and Lu, S.: Chemical character of precipitation and related particles and trace gases in the North and South of China, Journal of Atmospheric Chemistry, 67, 29-43, 10.1007/s10874-011-9201-6, 2010.

Kawamura, K., Steinberg, S., Ng, L., and Kaplan, I. R.: Wet deposition of low molecular weight mono- and di-carboxylic acids, aldehydes and inorganic species in Los Angeles, Atmospheric Environment, 35, 3917-3926, https://doi.org/10.1016/S1352-2310(01)00207-2, 2001.

Khuntong, S.: Ion Chromatographic Analysis of Monocarboxylic and Dicarboxylic Acids in Rainwater at Si Racha , Thailand Compared with Ogasawara Island and Tokyo , Japan,

Kieber, R. J., Peake, B., Willey, J. D., and Avery, G. B.: Dissolved organic carbon and organic acids in coastal New Zealand rainwater, Atmospheric Environment, 36, 3557-3563, https://doi.org/10.1016/S1352-2310(02)00273-X, 2002.

Kim, D. H., Takeda, K., Sakugawa, H., and Lee, J. S.: The photochemical reactions of iron species in rain and snow in Higashi-Hiroshima, Japan,

Lee, J. Y., Peterson, P. K., Vear, L. R., Cook, R. D., Sullivan, A. P., Smith, E., Hawkins, L. N., Olson, N. E., Hems, R., Snyder, P. K., and Pratt, K. A.: Wildfire Smoke Influence on Cloud Water Chemical Composition at Whiteface Mountain, New York, Journal of Geophysical Research: Atmospheres, 127, e2022JD037177, https://doi.org/10.1029/2022JD037177, 2022.

Liu, Y., Dong, X., Emmons, L. K., Jo, D. S., Liu, Y., Shrivastava, M., Yue, M., Liang, Y., Song, Z., He, X., and Wang, M.: Exploring the Factors Controlling the Long-Term Trend (1988–2019) of Surface Organic Aerosols in the Continental United States by Simulations, Journal of Geophysical Research: Atmospheres, 128, e2022JD037935, https://doi.org/10.1029/2022JD037935, 2023.

Löflund, M., Kasper-Giebl, A., Schuster, B., Giebl, H., Hitzenberger, R., and Puxbaum, H.: Formic, acetic, oxalic, malonic and succinic acid concentrations and their contribution to organic carbon in cloud water, Atmospheric Environment, 36, 1553-1558, https://doi.org/10.1016/S1352-2310(01)00573-8, 2002.

Peña, R. M., García, S., Herrero, C., Losada, M., Vázquez, A., and Lucas, T.: Organic acids and aldehydes in rainwater in a northwest region of Spain, Atmospheric Environment, 36, 5277-5288, https://doi.org/10.1016/S1352-2310(02)00648-9, 2002.

Pye, H. O. T., Nenes, A., Alexander, B., Ault, A. P., Barth, M. C., Clegg, S. L., Collett Jr, J. L., Fahey, K. M., Hennigan, C. J., Herrmann, H., Kanakidou, M., Kelly, J. T., Ku, I. T., McNeill, V. F., Riemer, N., Schaefer, T., Shi, G., Tilgner, A., Walker, J. T., Wang, T., Weber, R., Xing, J., Zaveri, R. A., and Zuend, A.: The acidity of atmospheric particles and clouds, Atmos. Chem. Phys., 20, 4809-4888, 10.5194/acp-20-4809-2020, 2020.

Sempéré, R. and Kawamura, K.: Low molecular weight dicarboxylic acids and related polar compounds in the remote marine rain samples collected from Western Pacific, Atmospheric Environment, 30, 1609-1619, https://doi.org/10.1016/1352-2310(95)00436-X, 1996.

Sigha-Nkamdjou, L., Galy-Lacaux, C., Pont, V., Richard, S., Sighomnou, D., and Lacaux, J. P.: Rainwater Chemistry and Wet Deposition over the Equatorial Forested Ecosystem of Zoétélé (Cameroon), Journal of Atmospheric Chemistry, 46, 173-198, 10.1023/A:1026057413640, 2003.

Sumari, S. M., Muhamad-Darus, F., Kantasamy, N., and Sinyaw, S. a. U.: Rainwater characterization at Global Atmospheric Watch in Danum Valley, Sabah, 2010 International Conference on Science and Social Research (CSSR 2010), 5-7 Dec. 2010, 479-484, 10.1109/CSSR.2010.5773824,

Sun, W., Zhang, G., Guo, Z., Fu, Y., Peng, X., Yang, Y., Hu, X., Lin, J., Jiang, F., Jiang, B., Liao, Y., Chen, D., Chen, J., Ou, J., Wang, X., Peng, P. a., and Bi, X.: Formation of In-Cloud Aqueous-Phase Secondary Organic Matter and Related Characteristic Molecules, Journal of Geophysical Research: Atmospheres, 129, e2023JD040355, https://doi.org/10.1029/2023JD040355, 2024.

Wang, Y., Sun, M., Li, P., Li, Y., Xue, L., and Wang, W.: Variation of low molecular weight organic acids in precipitation and cloudwater at high elevation in South China, Atmospheric Environment, 45, 6518-6525, https://doi.org/10.1016/j.atmosenv.2011.08.064, 2011.

Willey, J. D., Kieber, R. J., Williams, K. H., Crozier, J. S., Skrabal, S. A., and Brooks Avery, G.: Temporal Variability of Iron Speciation in Coastal Rainwater, Journal of Atmospheric Chemistry, 37, 185-205, 10.1023/A:1006421624865, 2000.

Xie, Z., Xiao, H., and Xu, Y.: Organic Acids in Sequential Volume-Based Rainwater Samples in Shanghai: Seasonal Variations and Origins, Atmosphere, 13, 1502, 2022.

Xu, G., Lee, X., and Lv, Y.: Urban and rural observations of carboxylic acids in rainwater in Southwest of China: the impact of urbanization, Journal of Atmospheric Chemistry, 62, 249-260, 10.1007/s10874-010-9151-4, 2009.

Zaveri, R. A., Easter, R. C., Fast, J. D., and Peters, L. K.: Model for Simulating Aerosol Interactions and Chemistry (MOSAIC), Journal of Geophysical Research: Atmospheres, 113, https://doi.org/10.1029/2007JD008782, 2008.

Zhang, Y. L., Lee, X. Q., and Cao, F.: Chemical characteristics and sources of organic acids in precipitation at a semi-urban site in Southwest China, Atmospheric Environment, 45, 413-419, https://doi.org/10.1016/j.atmosenv.2010.09.067, 2011.

Zhang, Z., Zhao, W., Hu, W., Deng, J., Ren, L., Wu, L., Chen, S., Meng, J., Pavuluri, C. M., Sun, Y., Wang, Z., Kawamura, K., and Fu, P.: Molecular characterization and spatial distribution of dicarboxylic acids and related compounds in fresh snow in China, Environmental Pollution, 291, 118114, https://doi.org/10.1016/j.envpol.2021.118114, 2021.

Zhao, W., Fu, P., Yue, S., Li, L., Xie, Q., Zhu, C., Wei, L., Ren, H., Li, P., Li, W., Sun, Y., Wang, Z., Kawamura, K., and Chen, J.: Excitation-emission matrix fluorescence, molecular characterization and compound-specific stable carbon isotopic composition of dissolved organic matter in cloud water over Mt. Tai, Atmospheric Environment, 213, 608-619, https://doi.org/10.1016/j.atmosenv.2019.06.034, 2019.

Zhu, Z., Liu, C.-Q., Wang, Z.-L., Liu, X., and Li, J.: Rare earth elements concentrations and speciation in rainwater from Guiyang, an acid rain impacted zone of Southwest China, Chemical Geology, 442, 23-34, https://doi.org/10.1016/j.chemgeo.2016.08.038, 2016.